Electronic Supplementary Material (ESI) for Journal of Materials Chemistry A.

Supplementary Information

Evolution of ferroelectric domains in methylammonium lead iodide and correlation with the performance of perovskite solar cells

Tobias Leonhard,[ab] Holger Röhm,[ab] Fabian J. Altermann,[c] Michael J. Hoffmann[ac] and Alexander Colsmann[ab]*

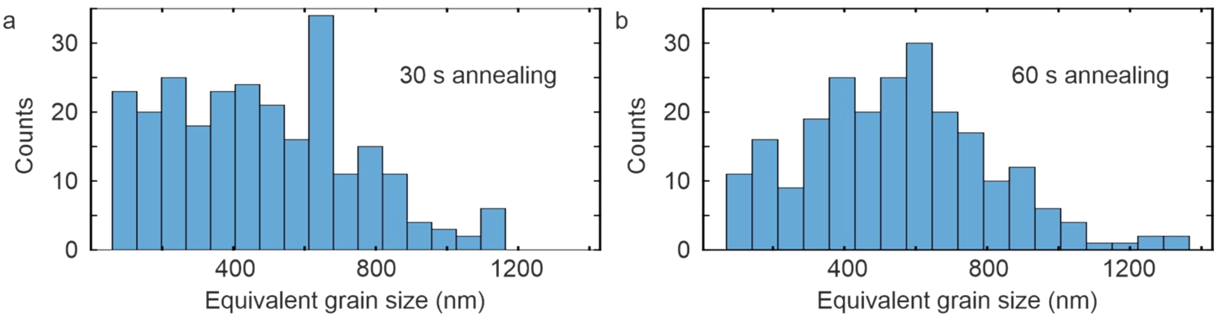

Figure S1. Statistical analysis of the grain size using the watershed based grain segmentation algorithm according to Rabbani et al.[1] (a) Relative number of grains, counted at three different positions of representative samples that were thermally annealed for 30 s. The grain size distribution confirms the visual impression that the sample exhibits a significant share of rather small grains. (b) After 60 s of thermal annealing, the number of smaller grains is reduced, quantitatively confirming the merging of small grains for larger grains.

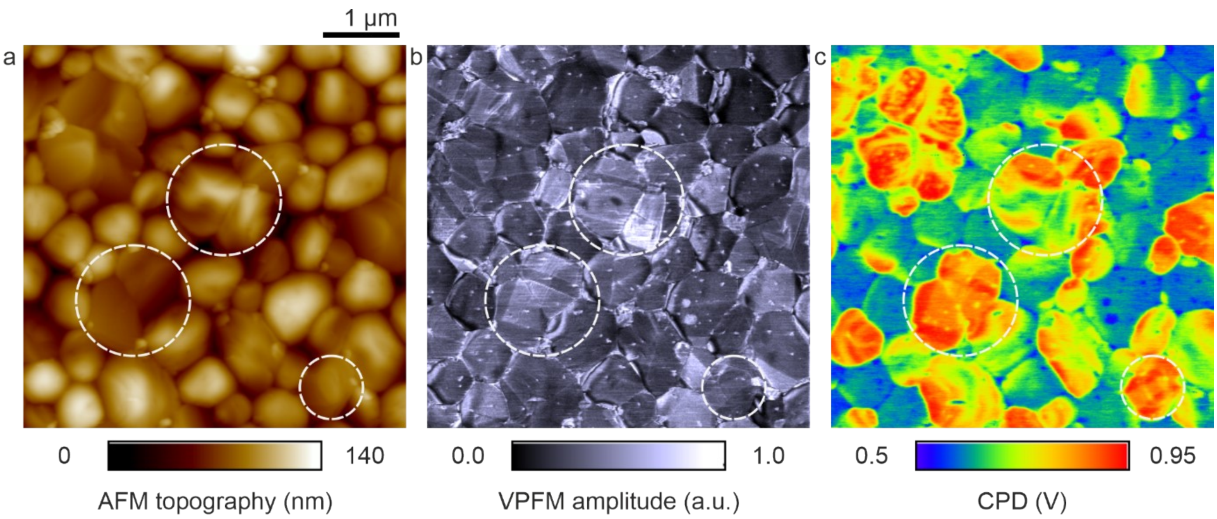

Figure S2. Modulation of the CPD by ferroelectric domains with out-of-plane polarization components. (a) Topography, (b) VPFM amplitude, (c) CPD. The trapezoidal vertical domains highlighted with white circles reduce the CPD by about 50 mV, which is in accordance with Figure 3 of the main manuscript, indicating a polarization pointing downwards (towards the substrate).

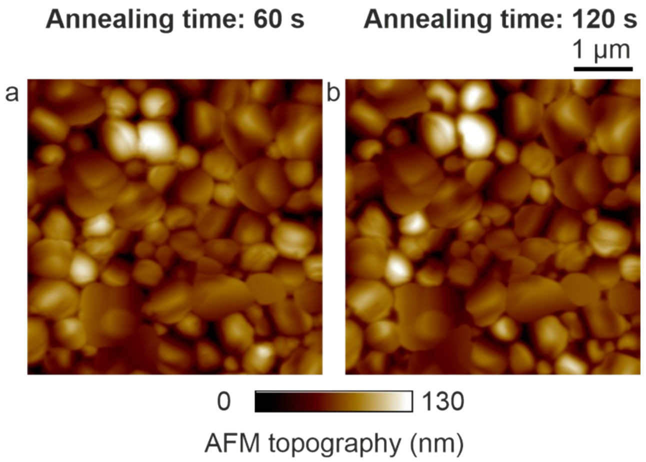

Figure S3. The topography of the sample in Figure 4 does not change from (a) before to (b) after the second annealing for 60s.

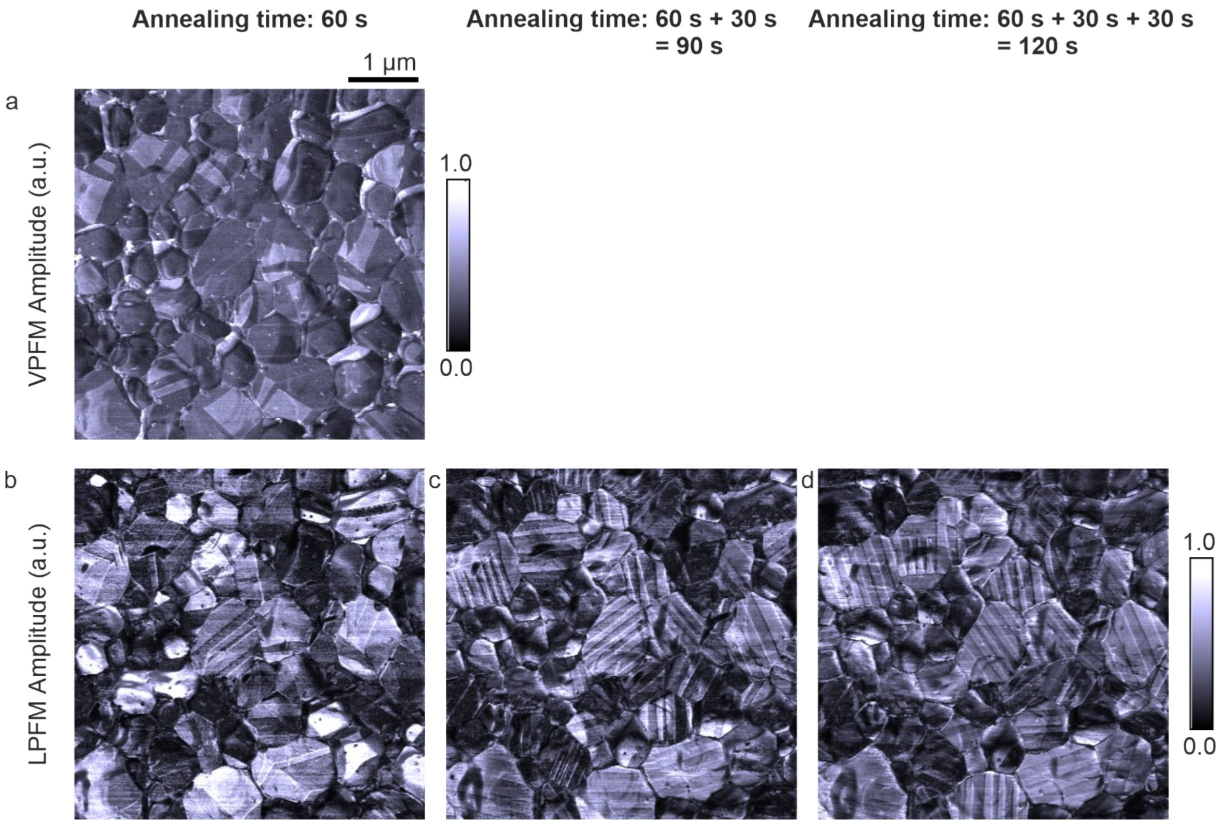

Figure S4. Evolution of ferroelectric domains. (a+b) Initial domain pattern after 60 s of annealing, monitored by VPFM and LPFM amplitude imaging. (c) Upon an additional annealing step of 30 s, more lateral domains emerge. (d) During the third annealing for 30 s, we observed only minor changes to the domain configuration, indicating an evolution towards a thermodynamically stable configuration.

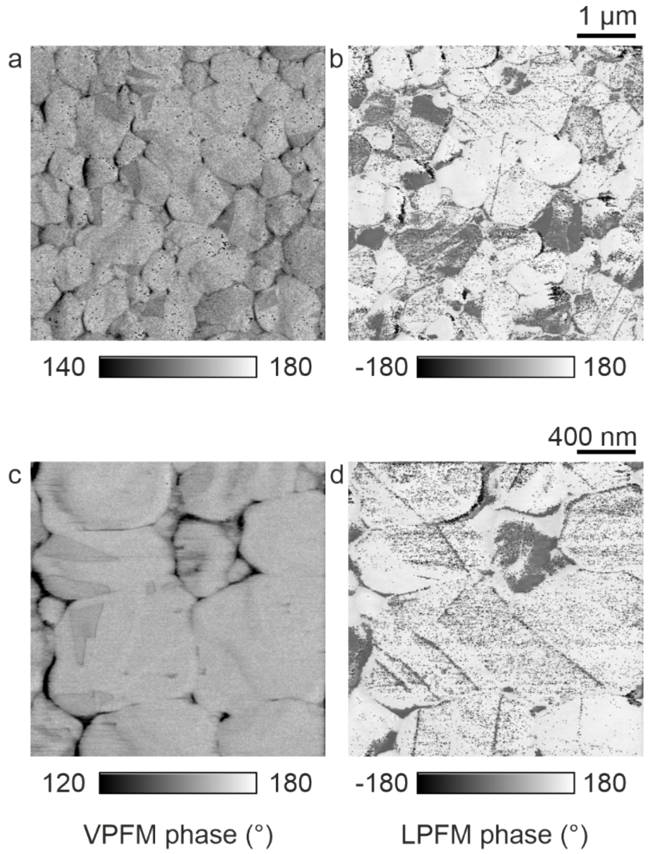

Figure S5. The PFM phase images support the PFM data of Figure 5, indicating (a) out-of-plane and (b) in-plane polarization components after sampling annealing for 60 s. (c+d) Magnification of VPFM and LPFM phase images.

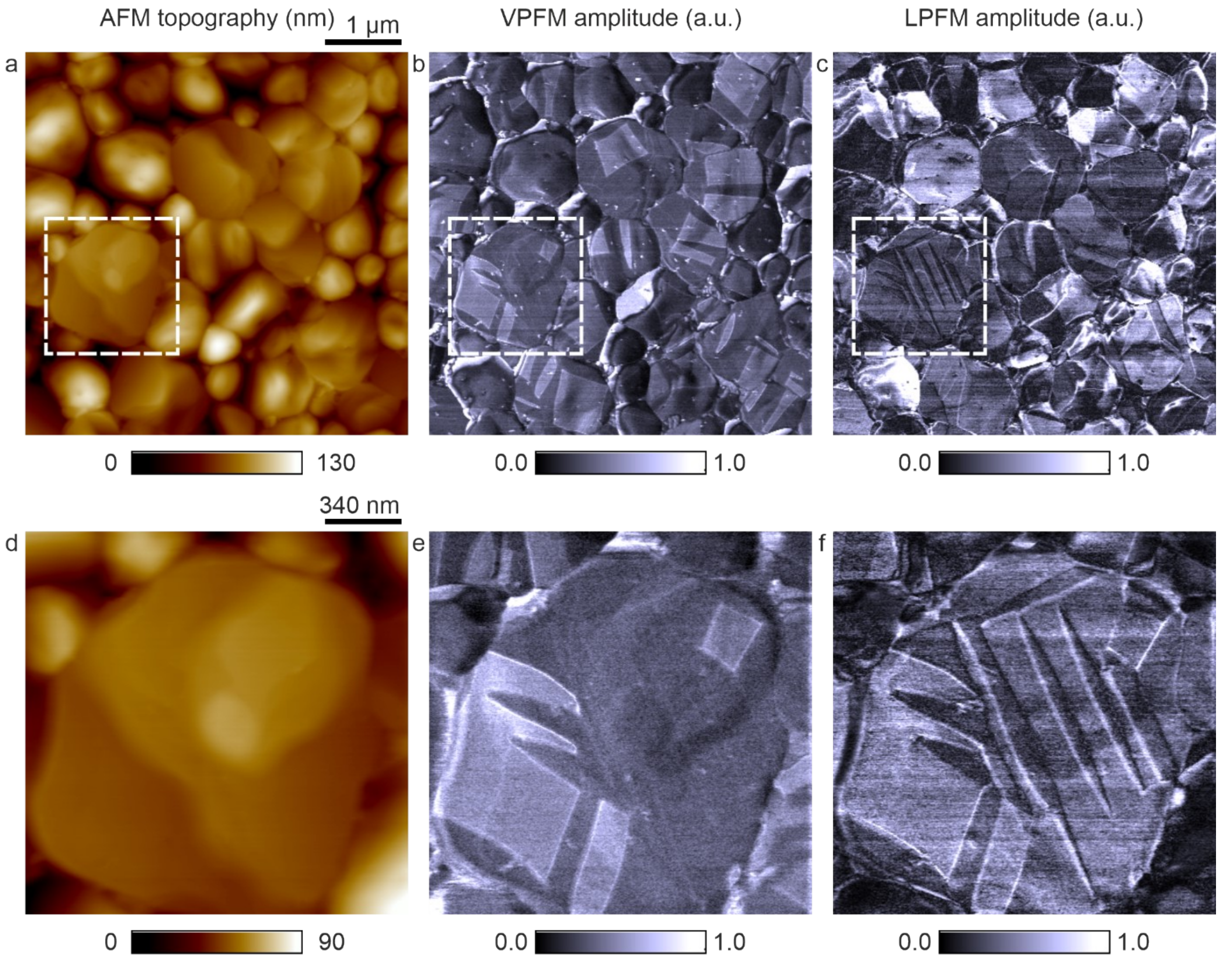

Figure S6. Configuration of vertical and lateral ferroelectric domains after 60 s of thermal annealing: (a) Topography, (b) VPFM amplitude and (c) LPFM amplitude. At this point in time during the domain evolution, grains are dominated by trapezoidal vertical domains with out-of-plane polarization. Yet, some areas of low VPFM amplitude show needle-like alternating domains in LPFM imaging. (d-f) The magnified marked image area reveals several indentations into the wall of the vertical domain which seemingly stem from in-plane polarized domains.

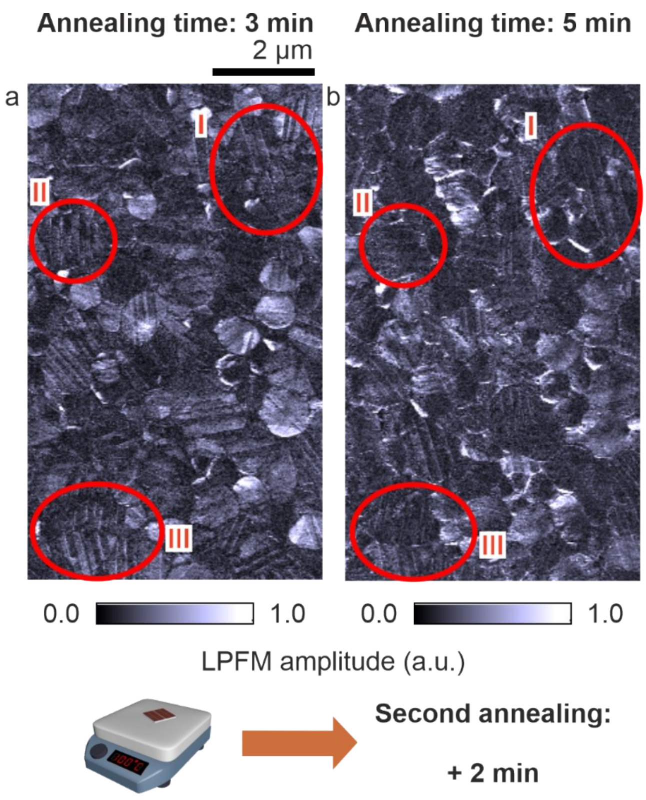

Figure S7. Formation and evolution of lateral ferroelectric domains. The LPFM amplitude images complete the dataset of Figure 6: (a) LFPM amplitude after 3 min of annealing. (b) LFPM amplitude after 5 min of annealing.

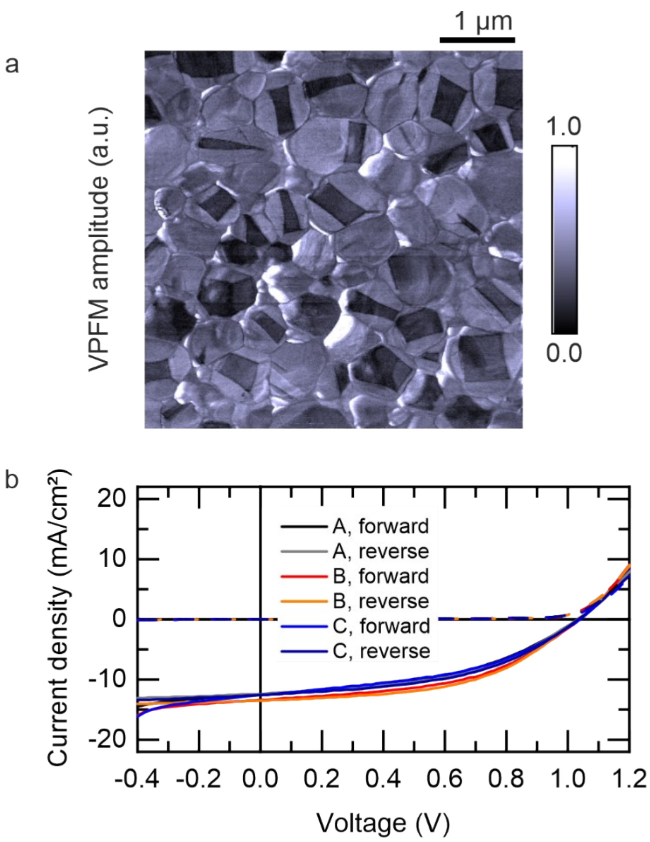

Figure S8. (a) The $MAPbI_3$ layer that was annealed for 30 s, is characterized by trapezoidal vertical domains in VPFM imaging. (b) After characterization by PFM, $PC_{71}BM$ and BCP layers as well as silver electrodes were added to complete the solar cells. The graph displays the J-V curves of three solar cells with out-of-plane polarization, all of which possess low fill factors.

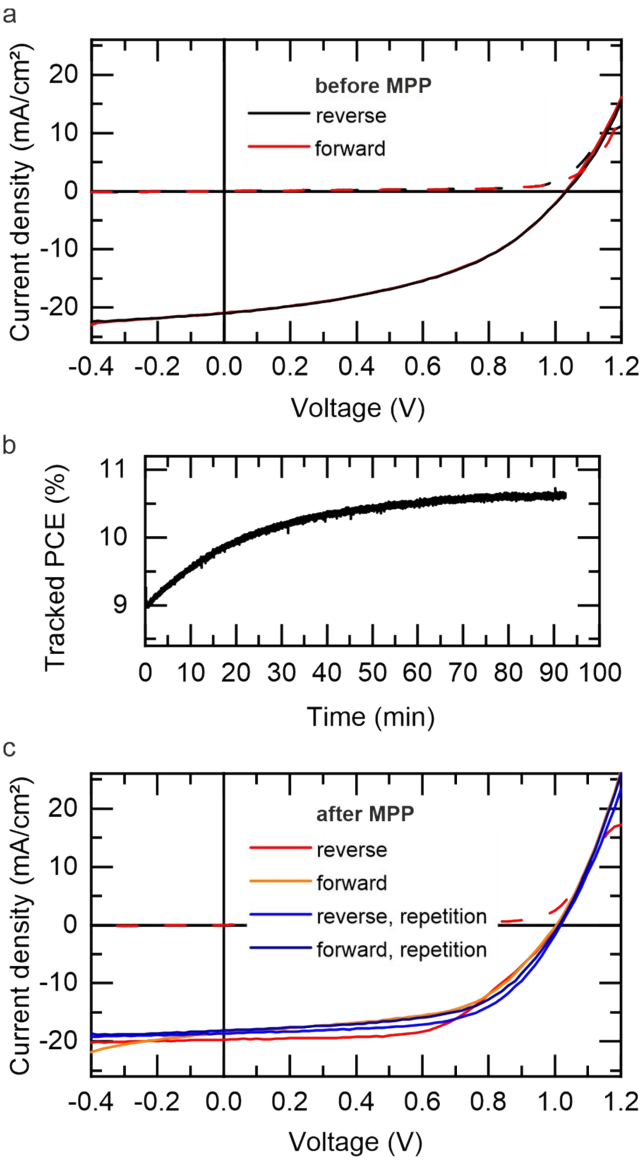

Figure S9. (a) J-V curve of a solar cell with a $MAPbI_3$ layer that was annealed for 30 s. (b) The PCE during MPP-tracking steadily increases during 90 min of measurement time. (c) The J-V curves after the MPP measurement possess reduced V_{OC} and J_{SC} and enhanced FF which may have their origin in a change of polarization orientation. Notably, the hysteresis of the solar cell is enhanced after exposure to light and electrical bias, possibly indicating the influence of mobile ions.

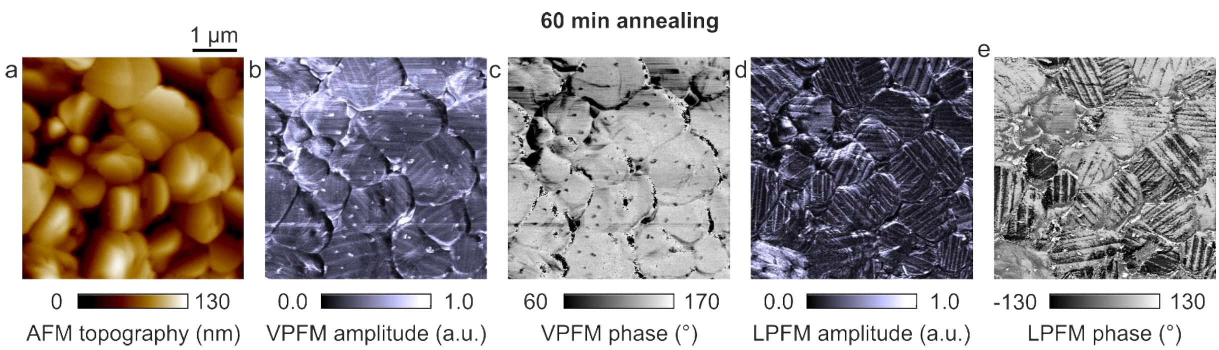

Figure S10. (a) Topography, (b) VPFM and (c) LPFM images of a sample fabricated with PbI_2 from Sigma Aldrich. The characteristic domain features and the grain size do not differ from the sample fabricated with PbI_2 from Alfa Aesar (sample 5, Figure 1).

Experimental Section

Annealing conditions: Figure S1: a) Sample 1-3: 5 s and then 30 s with Petri dish; b) Sample 4-6: 5s and then 60 s with Petri dish. Figure S2: 5 s and then 60 s with Petri dish. Figure S3: a+b) 5 s and then 60 s with Petri dish; c+d) additional annealing for 60 s with Petri dish (total annealing: 120 s). Figure S4: a+b) 5 s and then 60 s with Petri dish; c) additional annealing for 30 s with Petri dish (total annealing: 90 s); d) additional annealing for 30 s with Petri dish (total annealing: 120 s). Figure S5: 5 s and then 60 s with Petri dish. Figure S6+S7: 30 s with Petri dish. Figure S8: annealing procedure equals sample 5 in Figure 1.

References

1 A. Rabbani, S. Ayatollahi, *Special Topics & Reviews in Porous Media — An International Journal,* 2015, **6**, 71–89.